Neuron
Article

Rab GTPases-Dependent Endocytic Pathways Regulate Neuronal Migration and Maturation through N-Cadherin Trafficking

Takeshi Kawauchi,[1,2,3,*] Katsutoshi Sekine,[1] Mima Shikanai,[1] Kaori Chihama,[3] Kenji Tomita,[1] Ken-ichiro Kubo,[1] Kazunori Nakajima,[1] Yo-ichi Nabeshima,[3] and Mikio Hoshino[3,4]
[1]Department of Anatomy, Keio University School of Medicine, Tokyo 160-8582, Japan
[2]Precursory Research for Embryonic Science and Technology (PRESTO), Japan Science and Technology Agency (JST), Saitama 332-0012, Japan
[3]Department of Pathology and Tumor Biology, Graduate School of Medicine, Kyoto University, Kyoto 606-8501, Japan
[4]Department of Biochemistry and Cellular Biology, National Institute of Neuroscience, NCNP, Tokyo 187-8502, Japan
*Correspondence: takeshi-kawauchi@umin.ac.jp
DOI 10.1016/j.neuron.2010.07.007

SUMMARY

Although membrane trafficking pathways are involved in basic cellular functions, the evolutionally expanded number of their related family proteins suggests additional roles for membrane trafficking in higher organisms. Here, we show that several Rab-dependent trafficking pathways differentially participate in neuronal migration, an essential step for the formation of the mammalian-specific six-layered brain structure. In vivo electroporation-mediated suppression of Rab5 or dynamin to block endocytosis caused a severe neuronal migration defect in mouse cerebral cortex. Among many downstream endocytic pathways, suppression of Rab11-dependent recycling pathways exhibited a similar migration disorder, whereas inhibition of Rab7-dependent lysosomal degradation pathways affected only the final phase of neuronal migration and dendrite morphology. Inhibition of Rab5 or Rab11 perturbed the trafficking of N-cadherin, whose suppression also disturbed neuronal migration. Taken together, our findings reveal physiological roles of endocytic pathways, each of which has specific functions in distinct steps of neuronal migration and maturation during mammalian brain formation.

INTRODUCTION

The mammalian cerebral cortex evolutionally acquires a six-layered structure, which is essential for brain function, because its disruption results in brain malformations accompanied by mental retardation and/or seizure, such as lissencephaly and periventricular heterotopia (PVH), and is also associated with other neurological disorders, such as dyslexia and schizophrenia (Ayala et al., 2007; Gleeson and Walsh, 2000; Martinez-Cerdeno et al., 2006; Rakic, 2009). The formation of the six-layered cortex is largely dependent on the neuronal migration from the ventricular zone to the superficial layer of the cortical plate (Takahashi et al., 1999). During the migration, neurons exhibit various morphological changes, which are also thought to be associated with brain malformations (Kawauchi and Hoshino, 2008; LoTurco and Bai, 2006).

Postmitotic neurons, generated near the ventricle, first display a multipolar morphology in the lower part of the intermediate zone (multipolar cell accumulation zone; Tabata et al., 2009), and subsequently transform into bipolar-shaped locomoting neurons, which have a leading process, in the upper part of the intermediate zone. After migrating over a long distance along a radial glial fiber, which functions as a scaffold for migrating neurons, locomoting neurons change their migration mode into a terminal translocation mode and the leading processes mature into apical dendrites at the final phase of migration (Hatanaka and Murakami, 2002; Nadarajah et al., 2001; Rakic, 1972; Tabata and Nakajima, 2003). It has been reported that causative gene products of lissencephaly or PVH, such as Lis1 and DCX or filamin A, respectively, are involved in the regulation of microtubules and actin cytoskeleton (Ayala et al., 2007; Gleeson and Walsh, 2000; Kawauchi and Hoshino, 2008). Furthermore, we found that c-Jun N-terminal kinase (JNK) and cyclin-dependent kinase 5 (Cdk5) regulate the morphological changes of migrating neurons through the promotion of microtubule dynamics and actin reorganization (Kawauchi et al., 2003; Kawauchi et al., 2006). It has been also reported that the nuclear movement in the locomoting neurons is dependent on coordinated regulation of the cytoskeleton (Schaar and McConnell, 2005; Tsai and Gleeson, 2005). These findings indicate the essential roles of cytoskeletal regulation in the migration and morphological changes of neurons, and thereby in cortical layer formation and normal brain functions.

Recently, *ArfGEF2* was identified as a causative gene for PVH (Sheen et al., 2004). ArfGEF2/Big2 is localized at the Golgi apparatus and recycling endosome (Shin et al., 2004), implicating the possible involvement of membrane trafficking in cortical development. Genome-wide analysis showed that the ratio of human kinase genes that are predicted to be involved in endocytosis is quite high (Pelkmans et al., 2005), and that

membrane trafficking-related protein families are evolutionally expanded in humans (Pereira-Leal and Seabra, 2001). These facts suggest that, in addition to basic cellular functions, membrane trafficking may have important roles in higher organisms or mammals, including the formation of cerebral cortex with a complex six-layered structure. However, physiological roles of membrane trafficking in higher organisms are largely unknown.

Recent in vitro studies indicate that proper trafficking of integrin, a cell adhesion molecule involved in cell-to-extracellular matrix, is required for the migration of nonneuronal cells (Ezratty et al., 2009). It raises the possibility that membrane trafficking might play a role in neuronal migration during cerebral cortical development. However, the involvement of membrane trafficking in mammalian brain construction is still unclear. One of the major hurdles is that membrane trafficking is very complex cellular events as each cell contains many trafficking pathways that are regulated by numerous molecules, which makes it difficult to carry out in vivo experiments, including knockout analyses. Previously, we and others have established an in vivo gene transfer method, in utero electroporation, which allows us to analyze the functions of many molecules in vivo (Kawauchi et al., 2003; Saito and Nakatsuji, 2001; Tabata and Nakajima, 2001).

In this study, our analyses, by use of in utero electroporation, indicate the in vivo roles of endocytic pathways in neuronal migration and morphological changes during the development of cerebral cortex. We also found that, among many endocytic pathways, the Rab11-dependent recycling pathway and Rab7-dependent lysosomal degradation pathway regulate different steps of neuronal migration and maturation, suggesting that the sensitivities of neurons for each membrane trafficking pathway progressively change as they mature.

RESULTS

Involvement of Endocytosis in Neuronal Migration and Morphological Changes

To test the possible involvement of the endocytic pathways in cortical development, we first tried to express a dominant-negative form for dynamin I (K44A) (DN-Dyn-K44A), which inhibits almost all types of endocytosis (Altschuler et al., 1998; Damke et al., 1994; Praefcke and McMahon, 2004), in migrating neurons. Using in utero electroporation, a DN-Dyn-K44A-expressing vector was electroporated into embryonic cerebral cortices at embryonic day 14 (E14), and the brains were fixed at postnatal day 0 (P0), 5 days after electroporation. The electroporated cells were visualized with coexpressing EGFP. While control vector-electroporated cells migrated to reach the superficial layer of the cortical plate, DN-Dyn-K44A-expressing cells were stalled at the intermediate zone at P0 (Figure 1A). In addition, the number of EGFP-positive cells was decreased in DN-Dyn-K44A-electroporated cortices. When electroporated at E14, DN-Dyn-K44A-expressing cells migrate normally out of the VZ at E16 but many are missing at E17 probably due to cell death (Figure S1A). When a weaker form of DN-dynamin I (DN-Dyn-ΔPRD) (Ferguson et al., 2009; Okamoto et al., 1997) was expressed, DN-Dyn-ΔPRD-electroporated cells exhibited similar migration defects without a decrease in cell number (Figure 1A).

To elucidate the important roles of endocytosis in neuronal migration, we next applied a DN-Rab5 (S34N) (Rosenfeld et al., 2001). Expression of DN-Rab5 in primary cortical neurons delayed the endocytosis of Alexa594-conjugated transferrin (Figure S1F), suggesting that DN-Rab5 efficiently suppressed endocytosis in cortical neurons. The DN-Rab5-expressing vector was electroporated into E14 cerebral cortices, followed by fixation at P0. In contrast to control cells, many DN-Rab5-expressing cells were found stalled near the border between the intermediate zone and cortical plate (Figures 1A and S1B). Some of DN-Rab5-expressing cells had abnormal morphologies, including a disorganized leading process or round morphology at E17 (Figures S1C and S1D).

To confirm these results, we performed RNA interference (RNAi) experiments. Two short hairpin RNAs (shRNAs) for Rab5-expressing vectors effectively reduced the amount of endogenous Rab5 when transfected to primary cortical neurons (Figure 1F). These RNAi vectors were electroporated into E14 cerebral cortices. At P0, control scrambled (nontargeting) shRNA-expressing cells migrated normally to the superficial layer of the cortical plate, but Rab5-knockdown cells exhibited neuronal migration defects (Figure 1B). This migration defect was rescued by the coexpression of human wild-type Rab5 (wt-Rab5) with the Rab5-knockdown vector (Figure 1B). Similar to DN-Rab5-expressing cells, many Rab5-knockdown cells were stalled near the border between the intermediate zone and cortical plate, suggesting that Rab5-dependent endocytosis is required for entering the cortical plate.

Since migrating neurons exhibit various morphologies in the intermediate zone and these morphological changes may be associated with neuronal maturation and neurological disorders, we next analyzed the morphology of the Rab5-knockdown cells. Consistent with previous reports (Kawauchi and Hoshino, 2008), control migrating neurons exhibited multipolar morphology in the lower part of the intermediate zone and bipolar shape with a leading process in the cortical plate and the upper part of the intermediate zone (Figure 1C). In contrast, some Rab5-knockdown locomoting neurons displayed increased leading process branches (small arrowheads in Figure 1C; Figure 1D, $p < 0.02$, t test) or had abnormally thick trailing process (arrow in Figure 1C). Furthermore, Rab5-knockdown cells displayed a somewhat round morphology in the lower part of the intermediate zone (large arrowheads in Figure 1C). The ratio of multipolar cells was decreased significantly ($p < 0.02$, t test) and that of the round cells was increased in Rab5-shRNA-electroporated cortices ($p < 0.01$, t test), compared with control cortices (Figure 1E).

Rab5-knockdown cells expressed a neuronal marker, Hu protein, suggesting that the abnormal morphology and migration were not due to a defect in neuronal differentiation (Figure 1G). In addition, in the ventricular zone, where most of the cells are neural progenitors, no significant differences in the staining for proliferative markers, phospho-Histone H3 (PH3) (M phase) and Ki67 (late G1, S, G2, and M, but not G0, phases) were found between control and Rab5-shRNA-electroporated cortices at 1 day after electroporation (E15) (Figure S2B). To further confirm that the migration defects of Rab5-suppressing cells are not due to the defects in radial glia (neural progenitors), we constructed a neuron-specific Tα1 (α1-tubulin) promoter-driven DN-Rab5

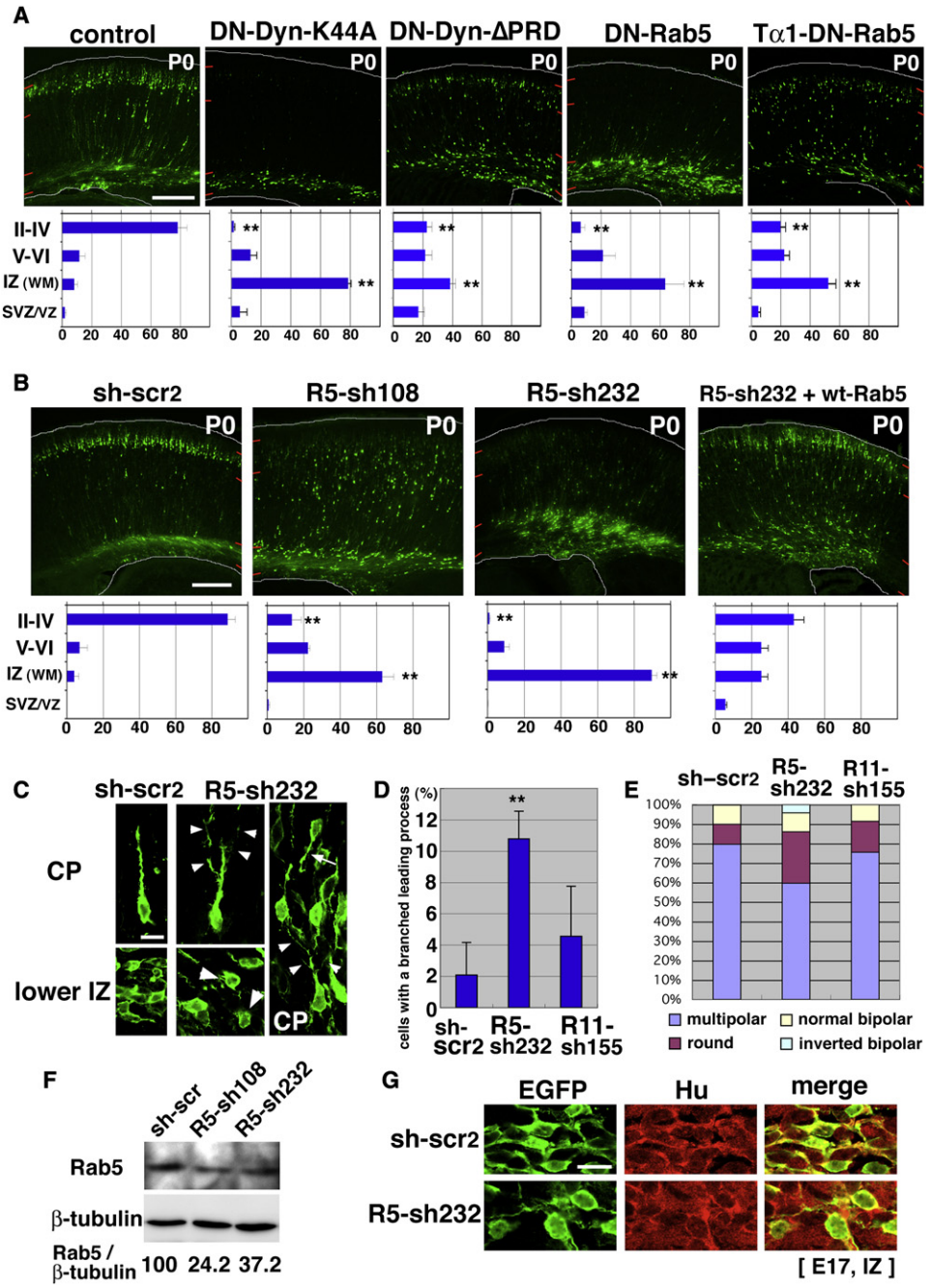

Figure 1. Inhibition of Endocytosis Disturbs Neuronal Migration

(A–C and G) Cerebral cortices at P0 (A and B) and E17 (C and G) electroporated with the indicated plasmids plus pCAG-EGFP at E14. White lines show pial or ventral surface, respectively. Short red bars indicate the borders between II-IV, V-VI, IZ, and SVZ/VZ. The lower graphs in (A) and (B) show the estimation of cell migration, which was carried out by recording fluorescence intensities of EGFP in distinct regions of the cerebral cortices using Leica SP5 software. Each bar represents the mean percentage of relative intensity ±SEM. n = 4 or 5 brains. II-IV, layers II-IV of the cortical plate; V-VI, layers V-VI of the cortical plate; IZ, intermediate zone; WM, white matter; SVZ/VZ, subventricular zone/ventricular zone. (C and G) High magnification of the indicated areas. CP, cortical plate; IZ, intermediate zone.

(D) The ratio of cells with a branched leading process in the CP ±SEM (n = 4 brains) (see Supplemental Experimental Procedures). Many more cells possessed branched leading processes in Rab5-shRNA-electroporated cortices ($p < 0.02$, t test), but not Rab11-shRNA-electroporated cortices ($p > 0.2$, t test).

(E) The ratio of cells with the indicated morphology in the IZ ±SEM (n = 4 brains) (see Supplemental Experimental Procedures). The ratio of the cells with multipolar morphology was decreased ($p < 0.02$, t test) and the ratio of the cells with round morphology was increased ($p < 0.01$, t test), when Rab5-shRNA was expressed.

(F) Immunoblot analysis of cortical neurons (2 DIV) transfected with the indicated plasmids with the indicated antibodies. Numbers represent ratios of Rab5/β-tubulin.

(G) Cortical sections were immunostained with EGFP and Hu.

**$p < 0.02$, t test (compared with control or sh-scr2). Scale bars: 200 μm in (A) and (B), 20 μm in (C) and (G). See also Figure S1.

vector to replace the ubiquitously expressed CAG promoter (Gloster et al., 1994). First, the Tα1-EGFP-expressing vector was coelectroporated with CAG-DsRed-expressing vector to estimate the strength of the promoter activity. At 3 days after electroporation (E17), no significant signals of EGFP were detected in the VZ as expected. In migrating neurons, EGFP expression levels were quite low, compared with DsRed (Figure S1E), although coelectroporation with CAG-EGFP and CAG-DsRed induced strong expression of both EGFP and DsRed (Kawauchi et al., 2003), suggesting that Tα1 promoter activity is very low. Consistent with this, when a high concentration of Tα1-DN-Rab5-expressing vector was coelectroporated with CAG-EGFP at E14, strongly transfected cells, but not EGFP-weak positive cells, showed migration defects similar to CAG-DN-Rab5 (Figure 1A), suggesting that the functions of Rab5 in postmitotic neurons are required for proper neuronal migration. We next electroporated Tα1-DN-Dyn-K44A into E14 cortices, but many EGFP-positive cells disappeared at P0. These results indicated that endocytosis plays important roles in neuronal migration and morphological changes, in addition to basic cellular functions, such as cell survival that was disturbed by DN-Dyn-K44A.

Rab11-Dependent Recycling Pathway Regulates Neuronal Migration

We next analyzed how Rab5-dependent endocytosis regulates neuronal migration. One possibility is that abnormal morphologies lead to the migration defects. A leading process with no or few branches is thought to be important for neuronal migration (Guerrier et al., 2009; Rakic, 1972). However, statistical analysis revealed that only about 30% of Rab5-knockdown neurons exhibited an abnormal morphology although the migration defects were present in the majority (Figures 1B–1E). Therefore, we further analyzed the downstream effects of Rab5-dependent endocytosis. It is known that Rab5 regulates both endocytosis and early endosome formation. From the early endosome (also called "sorting endosome"), there are many trafficking pathways, including recycling and lysosomal degradation pathways, each of which is regulated by a different subtype of Rab family protein (Figure 2H) (Pfeffer, 2001; Stenmark and Olkkonen, 2001; Zerial and McBride, 2001). Therefore, we perturbed each membrane trafficking pathway from the early endosome by means of in vivo functional suppression of Rab4 (fast recycling pathway), Rab11 (slow recycling pathway via recycling endosome), Rab7 (lysosomal degradation pathway), and Rab9 (retrograde transport to Golgi apparatus via late endosome). Dominant-negative forms for these Rab proteins were expressed in migrating neurons by using in utero electroporation at E14. At P0, introduction of DN-Rab4 (S22N), Rab7 (T22N), and Rab9 (S21N) did not have much effect on the migration of the locomoting neurons (Figures 2A, 2C, and 2D; data not shown), although the position of DN-Rab7-expressing cells was slightly but significantly lower than that of control (Figures 2C and 7A–7C).

In contrast, the expression of DN-Rab11 (S25N) significantly delayed neuronal migration in vivo (Figure 2B). Consistently, shRNA for Rab11, which efficiently reduced the protein level of endogenous Rab11 (Figure 2E), suppressed neuronal migration in the cortical plate (Figure 2F), but did not affect the expression of a neuronal marker, Hu protein (Figure 2G). In addition, the morphologies of radial glial fibers were not affected in both Rab11- and Rab5-shRNAs-electroporated cortices (Figure S2A). Coexpression of human wt-Rab11 with Rab11-shRNA restored neuronal positioning in the cortical plate (Figure 2F), suggesting that a Rab11-dependent recycling pathway is required for cortical neuronal migration.

Rab5 Suppression Affected Cell Adhesion

We next tried to identify the molecular cargo that is transported by the Rab5- and Rab11-dependent pathways. Although about 30% of Rab5-knockdown cells exhibited abnormal morphologies at 3 days after electroporation, many Rab5-knockdown cells formed a leading process. These cells seemed to attach to the radial glial fibers because their leading processes and radial glial fibers were intertwined (Figure 3A), but they could not migrate into the cortical plate (Figure 1B). Together with the observation that abnormally thick trailing processes of Rab5-knockdown cells also seemed to attach to the radial glial fibers (Figure 3A), this suggested that Rab5 suppression affects the cell adhesion between migrating neurons and radial glia, resulting in difficulty in detaching from the radial glial fiber at the cell rear.

To test this possibility, we performed a previously reported in vitro neuron-radial glia interaction assay (Gongidi et al., 2004) with some modifications. First, E15 cerebral cortices were dissociated and cultured in MEM (minimum essential medium) containing 10% horse serum. After a 7 day culture with two passages, F-actin-strong positive cells with fibroblast-like or elongated morphology were concentrated, and these cells expressed a radial glial marker, Nestin, but not a neuronal marker, Tuj1 (arrowheads in Figure 3B). Subsequently, primary cortical neurons transfected with Rab5-shRNA or control shRNA plus EGFP-expressing vectors were added to the Nestin-positive cells and co-cultured for 2 days. Almost all EGFP-positive cells were neurons as indicated by being Tuj1-positive and Nestin-negative (arrows in Figures 3B and S3A). EGFP-positive control neurons extended their processes along Nestin-positive cells, suggesting that adhesion molecule(s) may connect these cells (Figures 3C and S3A). Rab5-knockdown neurons also interacted with Nestin-positive cells, but they actively extended, branched and entangled their processes only when they attached to Nestin-positive cells (Figures 3C, S3A, and S3B). The length of the longest primary neurites overlapping with Nestin-positive cells was significantly increased, but total length of the longest primary neurites was not changed, compared with that of control (Figures 3D, 3E, and S3C). These data suggest that suppression of Rab5-dependent endocytosis promotes the cell adhesion between neurons and Nestin-positive cells.

Rab5 Regulates Subcellular Distribution of N-Cadherin

Cadherins and integrins are two major families of adhesion molecules. Both N-cadherin and β1-integrin were expressed in primary cortical neurons (Figure S4A). N-cadherin was observed to be localized near the plasma membrane and cytoplasmic punctuate structures, partially colocalizing with an early endosome marker, EEA1, and recycling endosome marker, Rab11, in primary cortical neurons (Figures S4B and S4C). In contrast,

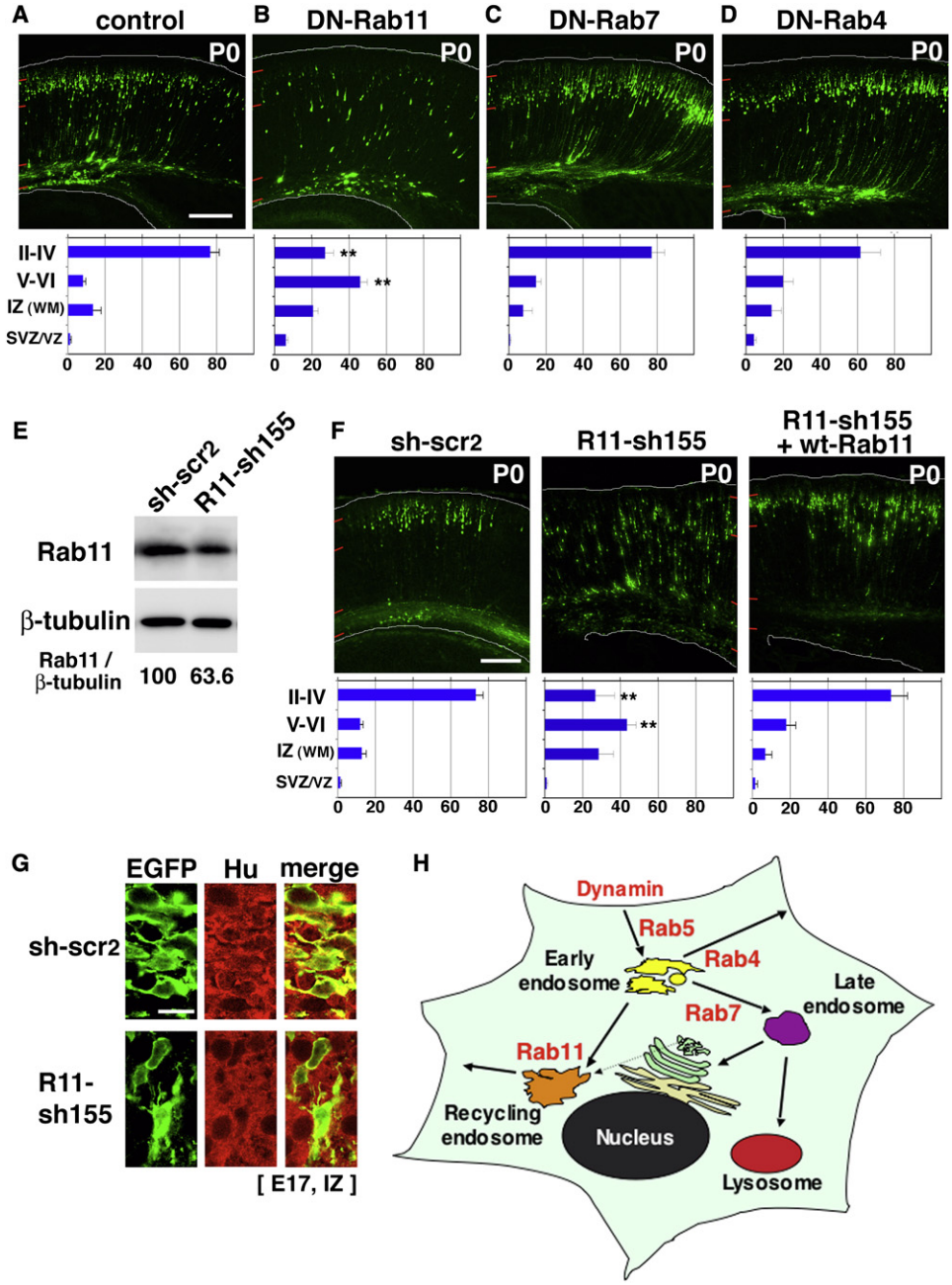

Figure 2. Suppression of Rab11 Affects Cortical Neuronal Migration

(A–D, F, and G) Cerebral cortices at P0 (A–D and F) and E17 (G) electroporated with the indicated plasmids plus pCAG-EGFP at E14. White lines show pial or ventral surface, respectively. Short red bars indicate the borders between II-IV, V-VI, IZ, and SVZ/VZ. The lower graphs in (A)–(D) and (F) show the estimation of cell migration (see Figure 1 legend).

(E) Lysates from primary cortical neurons (2 DIV) transfected with the indicated plasmids were subjected to immunoblot analyses with the indicated antibodies. The numbers indicate ratios of Rab11/β-tubulin.

(G) Frozen sections were immunostained with EGFP and Hu.

(H) Schematic drawing of endocytic pathways. Rab5 regulates endocytosis and early endosome dynamics. From the early endosome, there are many trafficking pathways: Rab4-dependent fast recycling pathways to plasma membrane, Rab11-dependent recycling pathways via recycling endosomes, Rab7-dependent degradation pathways to lysosomes.

**$p < 0.02$, t test (compared with control or sh-scr2). Scale bars: 200 μm in (A)–(D) and (F), 20 μm in (G). See also Figure S2.

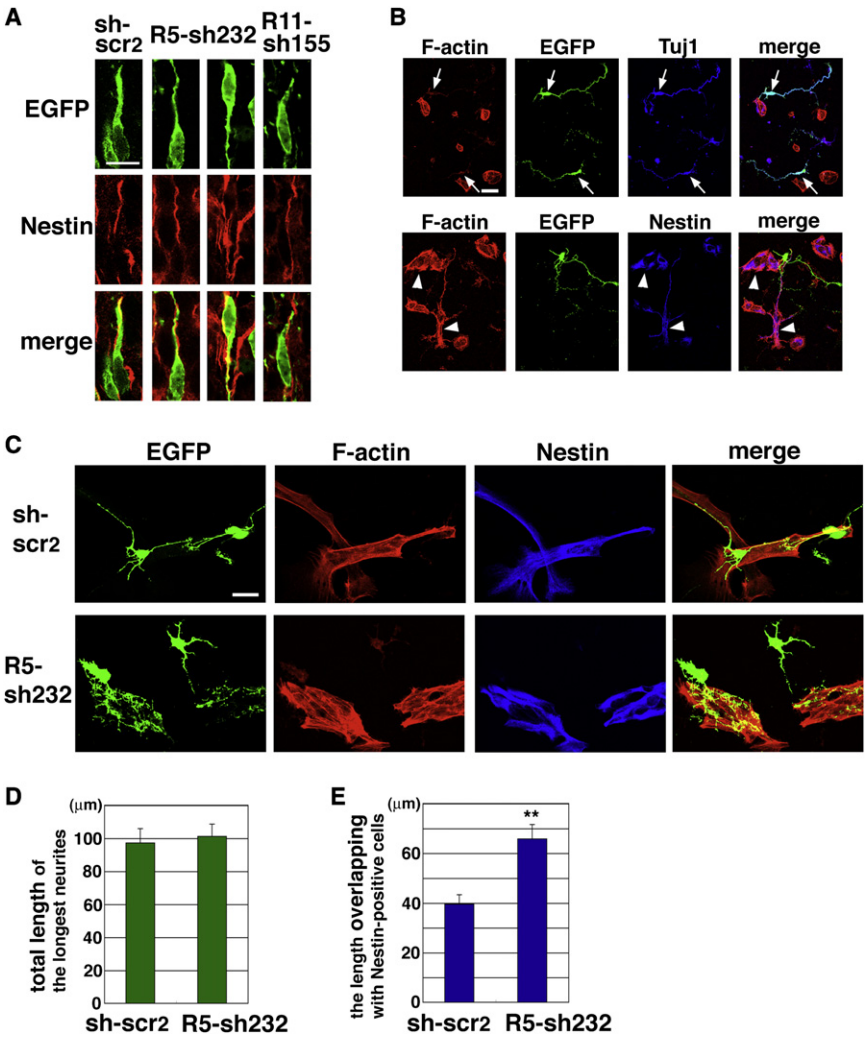

Figure 3. Rab5 Suppression Promotes Cell-Cell Interaction In Vitro

(A) Cerebral cortices at E17 electroporated with the indicated plasmids plus pCAG-EGFP at E14. Frozen sections of these brains were immunostained with EGFP and Nestin.

(B and C) Coculture of primary cortical neurons (2 DIV), transfected with sh-scr2 (B and upper panels in C) or R5-sh232 (lower panels in C) plus pCAG-EGFP, and Nestin-positive primary glia (9DIV) were immunostained with the indicated antibodies. Note that R5-sh232-transfected neurons actively extended and entangled their processes only when they attached to Nestin-positive cells.

(D and E) The average length ±SEM of the longest primary processes (not including branched secondary processes) of transfected neurons. Although the total length (the graph in D) was not changed ($p > 0.2$, t test), the length overlapping with Nestin-positive cells was significantly increased in R5-sh232-transfected neurons, compared with control ($p < 0.001$, t test, n = more than 50 cells).

**$p < 0.02$, t test (compared with sh-scr2). Scale bars: 10 μm in (A), 40 μm in (B), 25 μm in (C). See also Figure S3.

β1-integrin was partially colocalized with EEA1, but barely with Rab11 (Figures S4B and S4C).

We next analyzed the cell surface expression levels of these adhesion molecules in Rab5-knockdown cells by the use of fluorescence-activated cell sorter (FACS). Primary cortical neurons transfected with Rab5-shRNA or control shRNA plus EGFP-expressing vectors were treated with anti-N-cadherin or β1-integrin antibody and subjected to FACS analysis to examine the cell surface expression levels of these proteins on EGFP-positive cells. Knockdown of Rab5 resulted in about 10% increase of the surface levels of N-cadherin, but did not affect that of β1-integrin (Figure 4A) (the ratio of surface N-cadherin in Rab5-knockdown cells to that of control was 1.09 ± 0.03; $p < 0.02$, t test).

Although dissociated neurons barely migrate, they change their morphologies and elongate neurites, suggesting that cell surface adhesion molecules may actively be transported. Cell surface staining for N-cadherin using nonpermeabilized cortical neurons showed that the distribution of surface N-cadherin was gradually increased along neuronal processes in control cells (Figures 4B and 4C). Surface N-cadherin levels at distal or proximal regions of neuronal processes were higher than those of proximal regions or cell bodies, respectively (distal versus proximal: $p < 0.01$, proximal versus cell bodies: $p < 0.001$, t test, n = 52 cells). In contrast, surface N-cadherin levels at proximal and distal regions of neuronal processes were not significantly changed in Rab5-knockdown neurons ($p > 0.1$, t test, n = 54 cells) (Figures 4B and 4C). These in vitro data suggest that Rab5 regulates cell adhesion and surface distribution of N-cadherin in primary cortical neurons.

Immunohistochemical analyses showed that N-cadherin was expressed throughout cerebral cortex at E17 and found in both migrating neurons and radial glial fibers (Figures 4D, 4E, and S4D). Since our in vitro results showed that Rab5 suppression slightly increased surface levels of N-cadherin, we examined whether weak in vivo knockdown of N-cadherin can rescue the Rab5-knockdown phenotypes or not. When low concentrations (0.5 μg/μl) of shRNA for N-cadherin (NC-sh1023, see Figure 6B) were coelectroporated, the migration defects of Rab5-knockdown cells were partially restored (Figure 4F). These data suggest that Rab5-dependent endocytosis is involved in N-cadherin trafficking, which is required for proper neuronal migration in vivo.

Rab11 Is Required for N-Cadherin Trafficking

Our data suggest that, among many endocytic pathways, the Rab11-dependent recycling pathway is a main contributor to

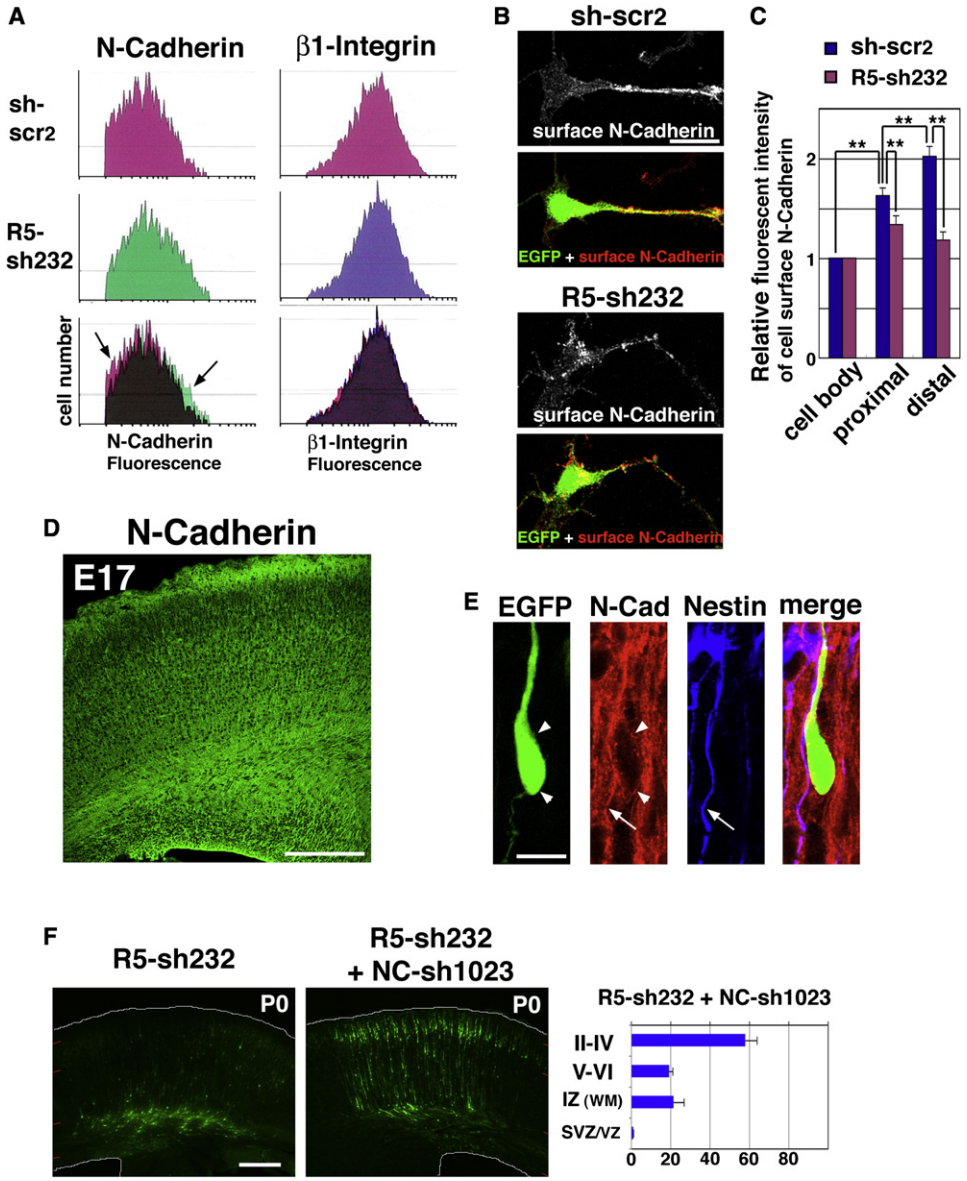

Figure 4. The Knockdown of Rab5 Perturbed the Distribution of Cell Surface N-Cadherin

(A) FACS analysis of primary cortical neurons transfected with the indicated plasmids. y axes show the cell number and x axes show the fluorescence intensity of N-cadherin (left panels) and β1-integrin (right panels). R5-sh232-transfected cells induced about 10% increase of the average fluorescent intensity of cell surface N-cadherin (arrows), but not β1-integrin.

(B and C) Nonpermeabilized primary cortical neurons (2 DIV) transfected with the indicated plasmids were immunostained with surface N-cadherin. Maximum projection images of ten Z-stack images (each interval is 0.7 μm) of the representative cells are shown in (B). The graph in (C) shows fluorescent intensities ±SEM of surface N-cadherin in the cell bodies or the proximal or distal regions of the longest neurites in transfected neurons, measured by the line scanning of Leica SP5 software. (Proximal region to cell body: $p < 0.01$, distal to proximal: $p < 0.01$, in control. Distal to proximal: $p > 0.1$, in R5-sh232. t test, n = more than 50 cells).

(D and E) E17 cerebral cortices immunostained with the indicated antibodies. Brain in (E) was eletroporated with pCAG-EGFP at E14 to visualize migrating neurons.

(F) Cerebral cortices at P0 electroporated with the indicated plasmids plus pCAG-EGFP at E14. The right graph shows the estimation of cell migration (see Figure 1 legend). The fluorescence intensities in the II-IV and IZ were significantly restored in brains coelectroporated with NC-sh1023 and R5-sh232, compared with R5-sh232-electroporated brains ($p < 0.001$ in both layers, t test).

Scale bars: 20 μm in (B), 10 μm in (E), 200 μm in (D) and (F). See also Figure S4.

neuronal migration. Because Rab5 suppression disturbed N-cadherin distribution, we next analyzed subcellular localization of N-cadherin in Rab11-suppressing neurons. Primary cortical neurons were transfected with DN-Rab11-expressing vectors, and subsequently fixed and stained with anti-N-cadherin or β1-integrin antibodies. Abnormal accumulation of

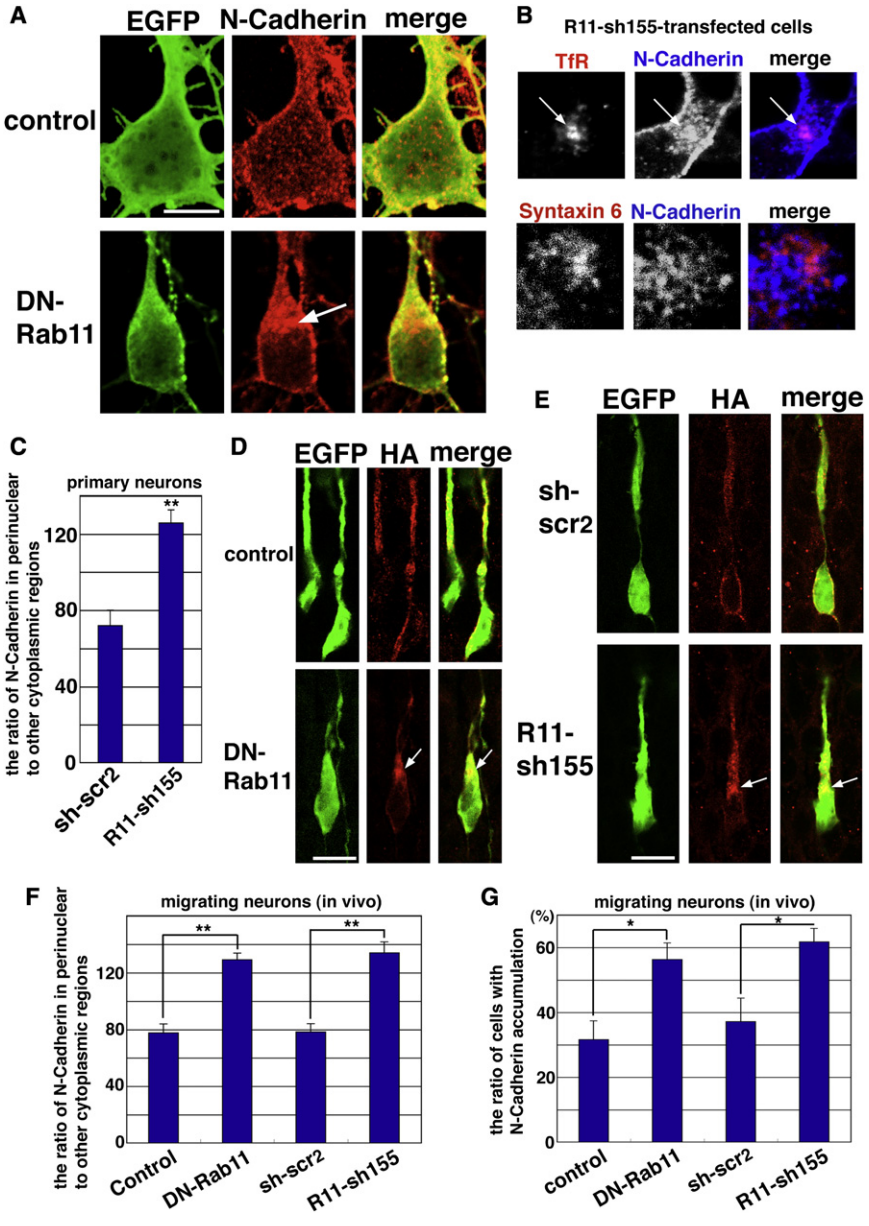

Figure 5. Involvement of Rab11-Dependent Recycling Pathway in N-Cadherin Trafficking

(A–C) Primary cortical neurons (2 DIV), transfected with the indicated plasmids, were immunostained with the indicated antibodies. Arrow in (A) shows abnormal accumulation of endogenous N-cadherin, which was partially colocalized with transferrin receptor (TfR) (arrows in B), but barely with Syntaxin 6. TfR and Syntaxin 6 are predominantly localized at recycling endosomes and *trans*-Golgi network, respectively.

(D–G) Cerebral cortices at E17 electroporated with the indicated plasmids plus HA-tagged wt-N-cadherin and pCAG-EGFP at E14. Frozen sections of these brains were immunostained with anti-EGFP and anti-HA antibodies to detect the localization of HA-tagged N-cadherin in migrating neurons. Arrows show abnormal accumulation of N-cadherin.

(C and F) The relative ratio of endogenous or HA-tagged N-cadherin staining signals/EGFP fluorescence in perinuclear regions to that of other cytoplasmic regions in primary cortical neurons (C) or migrating neurons in vivo (F), respectively. See Experimental Procedures for details.

(G) The ratio of cells with HA-N-cadherin accumulation in the migrating neurons electroporated with the indicated plasmids.

*$p < 0.05$, **$p < 0.02$, t test (compared with control or sh-scr2). Each error bar indicates the SEM from the mean. Scale bars: 5 μm in (A), 10 μm in (D) and (E). See also Figures S5 and S6.

N-cadherin, but not β1-integrin, was found in DN-Rab11-expressing neurons as visualized by coexpressed EGFP (Figures 5A and S5A). When DN-Rab5 was expressed, accumulation of N-cadherin in vesicular compartments was observed in some transfected cells in permeabilized conditions (Figure S5B), consistent with previous reports that Rab5 is involved in not only endocytosis but also early endosome formation (Pfeffer, 2001; Stenmark and Olkkonen, 2001; Zerial and McBride, 2001). Furthermore, expression of Rab11-shRNA in primary cortical neurons also induced accumulation of N-cadherin (Figures 5C and S6A–S6D). These subcellular accumulations of N-cadherin in Rab11-knockdown cells were colocalized with transferrin receptor, a marker for recycling endosomes, but barely with Syntaxin 6, a marker for *trans*-Golgi network (Figures 5B and S6C). Although Rab11 is involved in not only recycling but also post-Golgi trafficking of E-cadherin (Lock and Stow, 2005), our findings suggest that Rab11 mainly regulates the intracellular trafficking of N-cadherin via recycling endosomes in cortical neurons.

To examine the effects of Rab11 suppression on N-cadherin distribution in vivo, we weakly overexpressed HA-tagged wt-N-cadherin at E14 because it is difficult to divide the staining signals of endogenous N-cadherin derived from the electroporated migrating neurons and radial glial fibers or surrounding mature neurons. At E17, when most of the electroporated cells migrate in the cortical plate or intermediate zone, the distribution of the overexpressed protein in migrating neurons was observed by anti-HA antibody to allow discrimination of N-cadherin in the transfected cells from surrounding neurons or radial glial fibers. Expression of DN-Rab11 or Rab11-shRNA increased cells with intracellular accumulation of HA-tagged N-cadherin (Figures 5D, 5E, and 5G). To subtract the effects of cytoplasmic volume, HA-N-cadherin and EGFP fluorescent signals at the same regions were measured and the ratio of N-cadherin to EGFP fluorescent signals was calculated to evaluate "corrected HA-N-cadherin signals." The ratio of the corrected

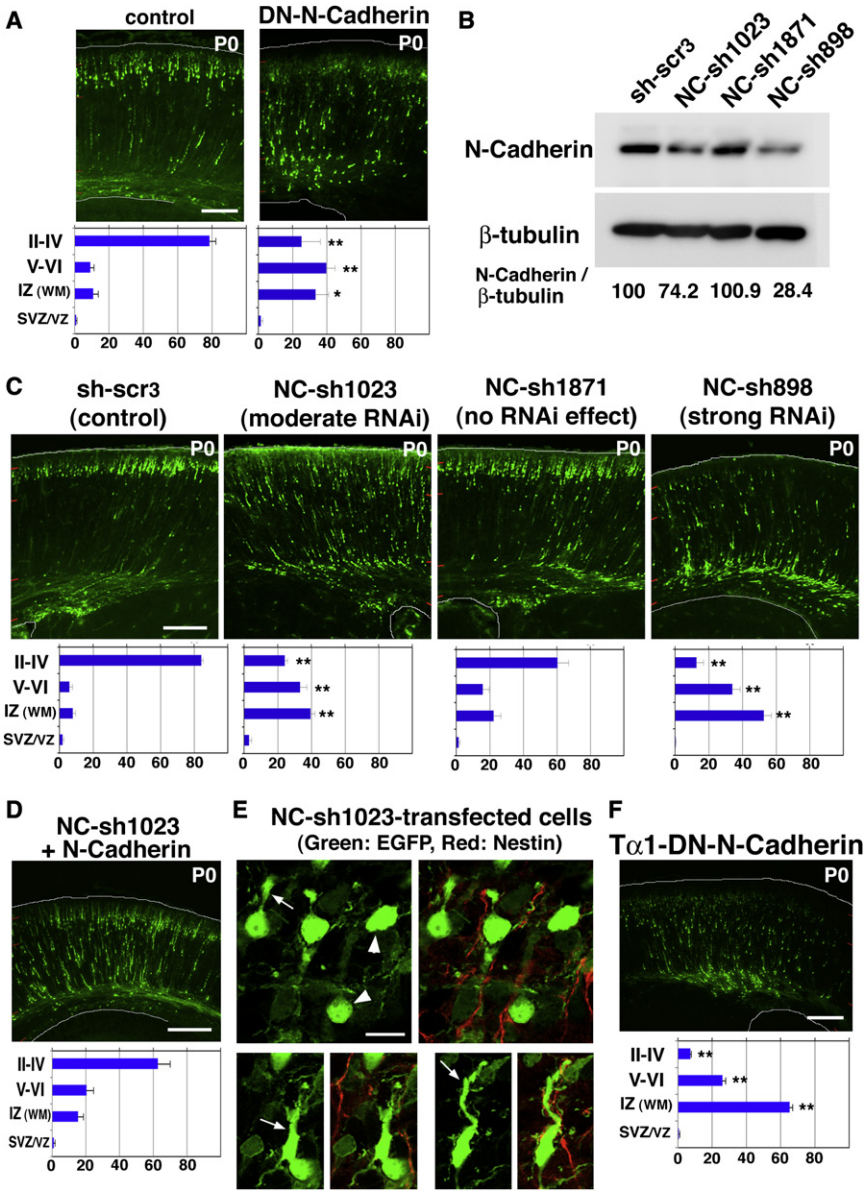

Figure 6. Suppression of N-Cadherin Affects Cortical Neuronal Migration

(A and C–F) Cerebral cortices at P0 (A, C, D, and F) or E17 (E) electroporated with the indicated plasmids plus pEGFP at E14. The lower graphs show the estimation of cell migration (see Figure 1 legend). (E) Cortical sections were immunostained with EGFP and Nestin. White arrows and arrowheads indicate abnormal morphologies of the leading processes and the round cells, respectively.

(B) Lysates from primary cortical neurons (2 DIV) transfected with the indicated plasmids were subjected to immunoblot analyses with the indicated antibodies. The numbers indicate the ratios of N-cadherin/β-tubulin.

**$p < 0.02$, t test (compared with control or sh-scr3). Each error bar indicates the SEM from the mean. Scale bars: 200 μm in (A), (C), (D), and (F); 10 μm in (E).

HA-N-cadherin signals in perinuclear regions to that of other cytoplasmic regions was increased in DN-Rab11 or R11-sh155-electroporated cells, compared with each control (DN-Rab11: $p < 0.0001$, R11-sh155: $p < 0.0001$, t test) (Figure 5F). These data suggest that Rab5- and Rab11-dependent endocytic recycling pathways play important roles in N-cadherin trafficking and neuronal migration along radial glial fibers.

N-Cadherin Regulates Cortical Neuronal Migration

To examine whether N-cadherin is required for neuronal migration, a DN-N-cadherin (Δ390)-expressing vector was electroporated into E14 cerebral cortices, and the electroporated brains were fixed at P0, 5 days after electroporation. DN-N-cadherin-expressing cells were abnormally located throughout the cortical plate and intermediate zone, whereas most of control cells reached the superficial layer of the cortical plate (Figure 6A). To confirm this, we designed shRNAs for N-cadherin. Three shRNAs exhibited different RNAi effects for endogenous N-cadherin in primary cortical neurons (Figure 6B); NC-sh1023, NC-sh1871, and NC-sh898 showed moderate, no, and strong RNAi effects, respectively. Introduction of the moderately effective NC-sh1023 into cerebral cortices resulted in disturbed neuronal migration (Figure 6C), and this abnormality was rescued by coexpressing HA-tagged N-cadherin with the NC-sh1023-resistant silent mutations (Figure 6D). Interestingly, in the rescue experiments, a small percentage of EGFP-positive cells was stalled at the border between the intermediate zone and cortical plate, and these stalled cells were strongly stained with anti-HA antibody, suggesting that too strong expression of N-cadherin also disturbed neuronal migration (data not shown).

While no effect was observed in brains treated with NC-sh1871 as expected, NC-sh898, which had a strong RNAi effect, caused severe migration defects resulting in the observation of many EGFP-positive cells near the border of the intermediate zone and cortical plate (Figure 6C). In the intermediate zone, the ratio of cells with round morphology was increased in NC-sh1023-electroporated cortices (47.6% ± 2.9%, $p < 0.001$, $n = 4$ brains [total 295 cells], t test) (Figure 6E), compared with control conditions (10.2% ± 1.4%, see Figure 1E). A part of N-cadherin-knockdown cells extended a leading process-like protrusion, but its morphology was abnormal (Figure 6E).

It has been reported that N-cadherin functions in the neural progenitors in the ventricular zone (Kadowaki et al., 2007;

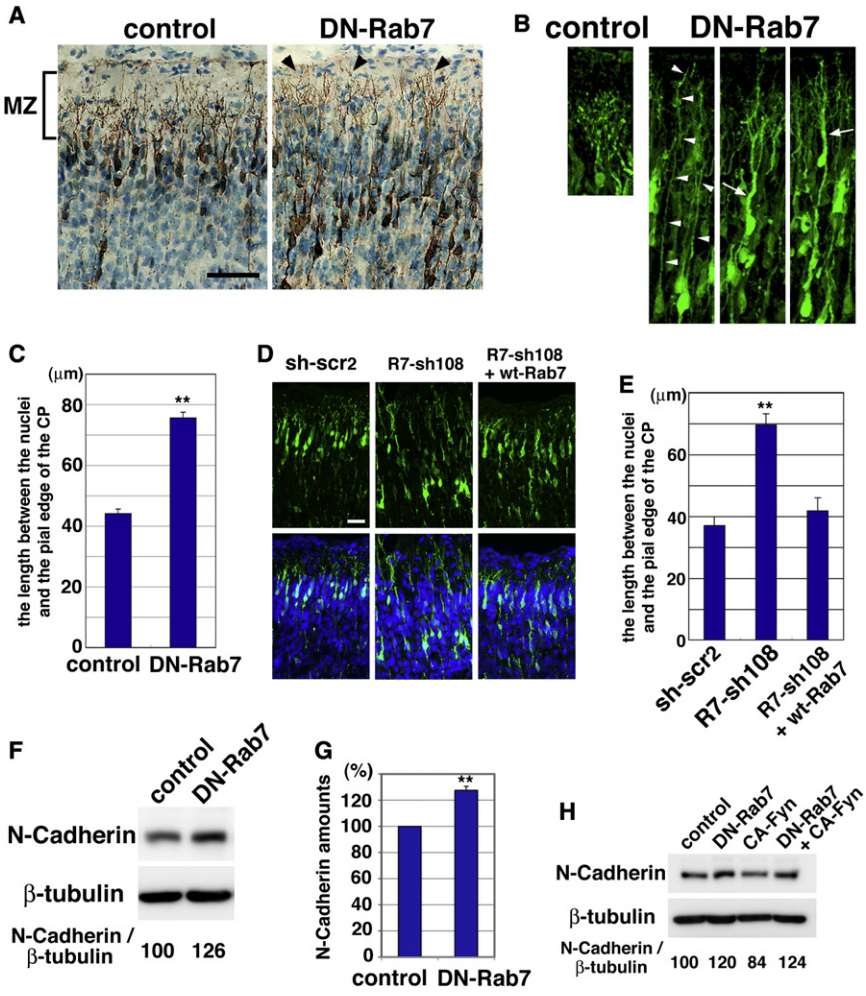

Figure 7. Rab7 Suppression Disturbs the Final Phase of Migration and Apical Dendrite Morphology

(A–E) P0 cerebral cortices electroporated with the indicated plasmids plus pEGFP at E14. Frozen sections were stained with anti-EGFP antibody (brown in A or green in B and D) and hematoxylin (blue in A) or DAPI (blue in D) for visualizing nuclei. (C and E) The graphs show the distances between the nuclei in EGFP-positive cells and the pial edge of the cortical plate. (C) n = 252 (control) or 256 (DN-Rab7) cells, $p < 0.001$ (t test). (E) n = 264 (sh-scr2) or 224 (R7-sh108) or 180 (R7-sh108 + wt-Rab7) cells. R7-sh108 ($p < 0.001$, t test), but not R7-sh108 + wt-Rab7 ($p > 0.2$, t test), significantly increased the distance.

(F and H) Immunoblot analysis of cortical neurons (2 DIV) transfected with the indicated plasmids with the indicated antibodies. The numbers indicate the ratios of N-cadherin/β-tubulin.

(G) The graph indicates the ratios of N-cadherin/β-actin. DN-Rab7 significantly increased N-cadherin protein levels (n = 4, $p < 0.001$, t test).

**$p < 0.02$, t test (compared with control or sh-scr2). Scale bars: 50 μm. See also Figure S7.

Zhang et al., 2010). Therefore, we constructed and electroporated a neuron-specific Tα1-promoter-driven DN-N-cadherin vector. At P0, 5 days after electroporation, the electroporated cells exhibited migration defects (Figure 6F), suggesting that the functions of N-cadherin in postmitotic neurons are required for neuronal migration. These results suggest that N-cadherin is one of the major target molecules of the Rab5- and Rab11-dependent recycling pathway and contributes to cortical neuronal migration along radial glial fibers.

Rab7-Dependent Degradation Pathway Is Involved in the Final Phase of Migration, Rather Than the Locomotion Mode

As described above, Rab7 suppression had little effect on neuronal positioning, but the distances from the nuclei of DN-Rab7-expressing cells to the pial edge of the cortical plate were significantly increased, compared with that of control cells at 5 days, but not 4 days, after electroporation (Figures 2C, 7A–7C, and S7A; data not shown). Knockdown of Rab7 also caused similar neuronal positioning defects near the top of the cortical plate, and this abnormality was restored by coexpressing wt-Rab7 with Rab7-shRNA (Figures 7D, 7E, and S7B). Although their somal positions were slightly lower than control, the apical (pial) processes of DN-Rab7-expressing cells reached the marginal zone (white arrowheads in Figure 7B) and were well branched, exhibiting features of mature apical dendrites (black arrowheads in Figure 7A). This suggests that the lower somal positioning was due to a defect in the final phase of migration rather than just delayed locomotion. Consistent with this, it is known that the final phase of neuronal migration is morphologically and molecularly different from the locomotion mode of migration, and thereby referred to as a specific migration mode termed "terminal translocation" (Nadarajah et al., 2001). Although we cannot completely exclude the possibility that the locomotion mode of migration was also affected, our data strongly suggest that the Rab7-dependent lysosomal degradation pathway specifically regulates the final phase of neuronal migration. Furthermore, the dendritic shafts in some DN-Rab7-expressing cells were thicker and longer than control (arrows in Figure 7B), and the dendritic branches were excessively elongated to reach the top of the marginal zone (arrowheads in Figures 7A and 7B).

To identify a target molecule of the Rab7-dependent degradation pathway, we focused on N-cadherin because we found that the staining signals for HA-tagged wt-N-cadherin were decreased near the top of the cortical plate (Figure S6E). Primary cortical neurons were transfected with DN-Rab7-expressing vector and subjected to immunoblot analysis with anti-N-cadherin antibody. The expression of DN-Rab7 slightly but significantly increased N-cadherin protein level (127.6% ± 3.0% of

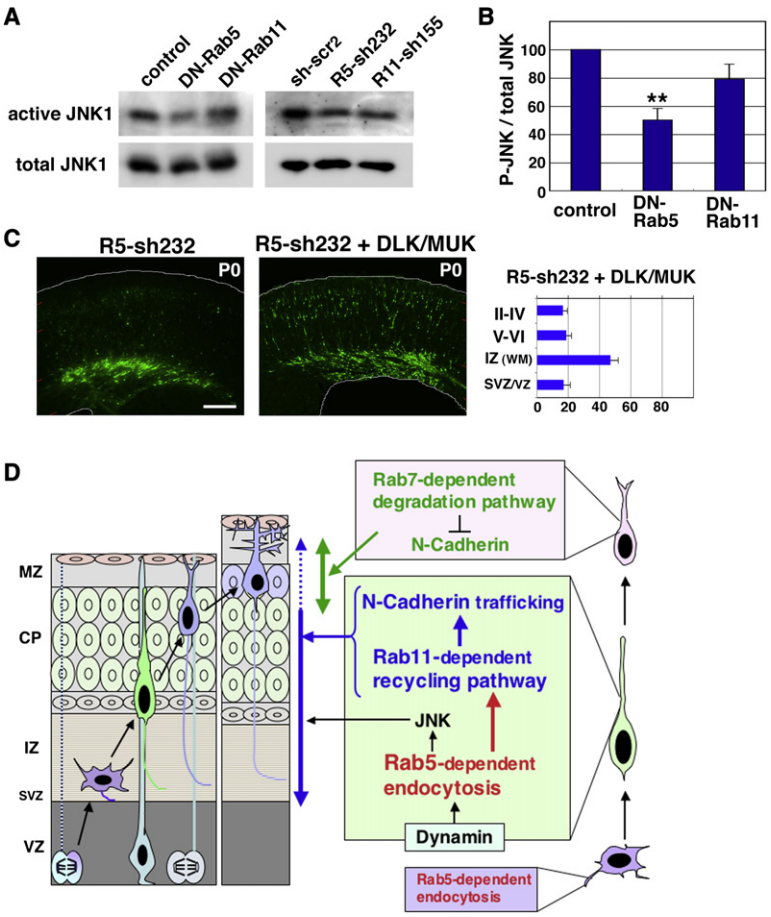

Figure 8. Rab5 Regulates JNK Activity as Well as Rab11-Dependent Recycling Pathway

(A and B) Immunoblot analysis of cortical neurons (2 DIV) transfected with the indicated plasmids with antiphosphorylated (active) JNK (upper panels) and anti-total JNK (lower panels) antibodies. The graph in (B) indicates the ratios of phosphorylated JNK/total JNK ±SEM (%). The suppression of Rab5 ($p < 0.01$, t test), but not Rab11 ($p > 0.05$, t test), significantly decreased JNK activity.

(C) Cerebral cortices at P0 electroporated with the indicated plasmids plus pCAG-EGFP at E14. The right graph shows the estimation of cell migration (see Figure 1 legend). The fluorescence intensities in II-IV and IZ were slightly but significantly restored in brains coelectroporated with CAG-DLK/MUK and R5-sh232, compared with R5-sh232-electroporated brains ($p < 0.01$ in both layers, t test). Scale bar: 200 μm.

(D) Neurons exhibit various morphological changes during the migration and maturation. Rab5-dependent endocytosis and Rab11-dependent recycling pathway that may be downstream of Rab5, are required for the entrance into the cortical plate and the migration of locomoting neurons (green cell in right) through the trafficking of N-cadherin. In contrast, Rab7-dependent lysosomal degradation pathway is involved only in the final phase of neuronal migration and dendrite morphology (light pink cells in right).

See main text and Figure S8.

control samples, $p < 0.001$, t test) (Figures 7F and 7G). During the final phase of migration, the activity of Fyn, a Src family kinase, is thought to be increased in response to Reelin signals, which is required for the terminal translocation (Olson et al., 2006; Tissir and Goffinet, 2003), although Fyn activity is also required for the locomotion mode or early phase of neuronal migration (Nishimura et al., 2010). When a constitutive active form for Fyn (CA-Fyn) was expressed in primary cortical neurons, the protein levels of N-cadherin were slightly decreased (84.9% ± 1.4% of control samples, $p < 0.01$, t test); this reduction of N-cadherin was restored by co-expression of DN-Rab7 with CA-Fyn (Figure 7H). These data suggest that, at least in part, N-cadherin is degraded by the Rab7-dependent lysosomal pathway in response to Fyn activity.

Suppression of Rab5, but Not Rab11, Decreased JNK Activity

A series of our experiments suggested that Rab5- and Rab11-dependent endocytic recycling pathways regulate neuronal migration along radial glial fibers through the trafficking of N-cadherin whereas Rab7-dependent degradation pathways are involved in the degradation of N-cadherin and the final phase of neuronal migration (Figure 8D). However, Rab5 inhibition exhibited stronger effects on neuronal migration than that of Rab11, implying that Rab5 plays other roles in neuronal migration, in addition to Rab11-dependent N-cadherin recycling. To test this possibility, we examined the activities of several kinases in DN-Rab5-expressing cells and found that DN-Rab5 decreased the active phosphorylated form of JNK, but not that of Erk1/2 or focal adhesion kinase at Ser732 that is phosphorylated by Cdk5 (Kawauchi et al., 2005; Xie et al., 2003), in primary cortical neurons (Figures 8A, 8B, and S8A). In contrast, DN-Rab11 did not significantly change the phosphorylation of JNK (Figures 8A and 8B), suggesting that Rab5 may regulate JNK activity independent of Rab11. Because JNK is known to regulate neuronal migration (Kawauchi et al., 2003), we examined whether Rab5-mediated JNK activation is also required for proper neuronal migration. To test this, we tried to increase JNK activity in Rab5-knockdown cells by means of overexpression of DLK/MUK, an upstream MAPKKK for JNK (Hirai et al., 2002). Interestingly, coexpression of DLK/MUK partially, but not fully, rescued the migration defects of Rab5-knockdown cells (Figure 8C), suggesting that Rab5 regulates JNK activity as well as Rab11-dependent recycling of N-cadherin to promote neuronal migration.

One of the major upstream regulators for JNK is Rac1, whose activity is controlled by Rab5 in HeLa cells and mouse embryonic fibroblasts (Palamidessi et al., 2008). However, inhibition of Rab5 did not significantly change Rac1 activity in cortical neurons at least as deduced from a GST-PAK1 pull-down assay (Rac1 activation assay, see Supplemental Experimental Procedures), and expression of Rac1 (F28L), a fast cycling mutant for Rac1, did not rescue the phenotype of Rab5 suppression (Figures S8B–S8E).

DISCUSSION

While brain function is dependent on the trafficking of synaptic vesicles, brain construction, including neurite extension and neuronal migration, is thought to be dependent on the proper regulation of microtubules and actin cytoskeleton, rather than membrane trafficking. In this study, we provide evidence that endocytosis and its downstream endocytic pathways play essential roles in neuronal migration and morphological changes during cerebral cortical development prior to synaptogenesis. Our findings also shed light on the physiological significance of membrane trafficking pathways in higher organisms, as their in vivo roles were largely unknown.

It is known that there are many endocytic pathways from the early endosome, such as fast and direct recycling pathways to plasma membrane, slow recycling pathways via recycling endosomes, degradation pathways to lysosomes, and retrograde transport to Golgi apparatus via late endosome, and these pathways are known to be regulated by different Rab family proteins (Pfeffer, 2001; Stenmark and Olkkonen, 2001; Zerial and McBride, 2001) (Figure 2H). Using in utero electroporation-mediated functional suppression for each Rab protein, we found that the Rab5-dependent endocytosis and Rab11-dependent slow recycling pathway regulates cortical neuronal migration, mainly the locomotion mode of migration, through the trafficking of N-cadherin (Figure 8D). In addition, our experiments also showed that the Rab7-dependent lysosomal degradation pathway is required for the final phase of migration and, partly, for apical dendrite maturation. These findings indicate that each membrane trafficking pathway differentially regulates distinct steps of neuronal migration and maturation, in addition to basic cellular functions, such as cell survival, in mouse cerebral cortex.

Rab5 suppression increased total cell surface N-cadherin and cell adhesion but decreased the localization of surface N-cadherin at the distal regions of the neuronal processes, suggesting that Rab5-dependent endocytosis regulates the trafficking of N-cadherin toward the distal tips of neuronal processes. Furthermore, Rab11 inhibition perturbed the intracellular trafficking of N-cadherin via recycling endosomes. Although Rab5 suppression exhibited much stronger effects compared with the others, in vivo suppression of Rab5 or Rab11 or N-cadherin caused similar neuronal migration defects. Together with our observation that too strong expression of N-cadherin also disturbed neuronal migration, these findings suggest that Rab5- and Rab11-dependent recycling of N-cadherin from trailing processes to the cell front may be important for the locomotion mode of migration along radial glial fibers. This hypothesis is also supported by our findings that some Rab5-knockdown neurons had an abnormally thick trailing process, in which N-cadherin was also localized (data not shown). It has been reported that blocking endocytosis, by the expression of DN-dynamin II, leads to defects of tail retraction in migrating fibroblasts (Ezratty et al., 2005), which may resemble the effects of Rab5 knockdown in migrating neurons. Furthermore, another very recent report using nonneuronal cells showed that endocytosis-mediated trafficking of integrin is required for cell migration (Ezratty et al., 2009). Thus, in addition to cytoskeletal regulation, the endocytosis and subcellular trafficking of cell adhesion molecules may have general roles in cell migration.

We could not observe the increase of surface β1-integrin level in Rab5-suppressed primary cortical neurons in our experimental conditions. However, we cannot completely exclude the possibility that integrins may be transported through Rab5- and/or Rab11-dependent endocytic pathway, because the primary cortical neurons in our experiments were cultured on poly-D-lysine-coated dishes without any extracellular matrices, such as fibronectin and laminin, which bind and activate integrins. In fact, recent in vitro studies revealed that trafficking of integrins are essential for the migration of cultured nonneuronal cells (Ezratty et al., 2009; Nishimura and Kaibuchi, 2007; Teckchandani et al., 2009). In addition, several precedent reports indicated cooperative roles of cadherin and integrin in nonneuronal cells (Shintani et al., 2008; Yano et al., 2004). These data implicated that Rab5- and Rab11-dependent recycling pathways may play important roles in the trafficking of many membrane-associated molecules, including not only N-cadherin but also integrins, and thereby regulate cortical neuronal migration.

The suppression of Rab5, but not Rab11, partly decreased JNK activity, and overexpression of DLK/MUK slightly restored the migration defects of Rab5-knockdown cells. In contrast, Rab5 had little effect on the activity of Rac1, one of main upstream regulators of JNK. Since many upstream pathways for JNK are reported (Huang et al., 2004; Raman et al., 2007), Rab5 may be involved in some of these pathways likely in a Rac1-independent manner. Rab5-knockdown phenotypes were also rescued by coexpression of weak shRNA for N-cadherin, suggesting that Rab5 regulates both JNK and N-cadherin trafficking. However, we cannot exclude the possibility that these observations are derived from indirect effects because suppression of one cell adhesion molecule sometimes affects the activity of the others. The leading processes of N-cadherin-knockdown cells tended to adhere with each other, suggesting that other adhesion molecule(s) may be activated. Proper protein levels and distribution of N-cadherin may regulate the activities of many adhesion molecules to control the overall cell adhesion properties of migrating neurons.

Our data showed that Rab7 is required for the final phase of migration, rather than the locomotion mode (Figure 8D). In some regions of the cortex, the position of DN-Rab4-expressing cells also seemed to be slightly lower than that of controls at 5 days after electroporation (Figure 2D). These data suggest that the final phase of migration exhibits different sensitivities for membrane trafficking pathways. We recently reported that functional suppression of PKCδ caused a phenotype similar to Rab7 suppression (Nishimura et al., 2010). Consistently, a recent study reported that PKCδ acts upstream of lysosomal organization (Romero Rosales et al., 2009), implicating that PKCδ might act as an upstream of Rab7-dependent lysosomal degradation pathway to regulate the final phase of migration. We also found that Fyn activity, which should be enhanced at the final phase of migration by Reelin signal (Tissir and Goffinet, 2003), promoted the degradation of N-cadherin protein at least in part in a Rab7-dependent manner, suggesting that N-cadherin is a candidate for the target molecule of the Rab7-dependent degradation pathway to regulate the final phase of migration. An attractive

hypothesis is that increased Fyn activity changes N-cadherin transport from Rab11-dependent recycling pathway into lysosomal degradation pathway at the final phase of migration, which may induce the transformation from the locomotion mode of migration along radial glial fibers to the radial fiber-independent terminal translocation mode of migration. However, the effects of DN-Rab7 and CA-Fyn on N-cadherin protein levels did not appear very strong, suggesting that although N-cadherin is one important target of the Rab7-dependent degradation pathway, there may be other important target molecules of this process.

EXPERIMENTAL PROCEDURES

Plasmids and Antibodies

Plasmids and primary antibodies used in this study were described in the Supplemental Experimental Procedures.

In Utero Electroporation

Animals were handled in accordance with guidelines established by Kyoto University and Keio University. All electroporations in this report were performed on E14 embryos. In utero electroporation and quantification of EGFP fluorescence intensities in various regions of electroporated cerebral cortices were performed as described previously (Kawauchi et al., 2003). See the Supplemental Experimental Procedures for details.

Quantitative Analysis for the Ratio of Cells with Different Morphology

The morphology of migrating neurons was analyzed on frozen sections of cerebral cortices at E17, 3 days after electroporation. The numbers of the cells with multipolar or round or normal bipolar or inverted bipolar morphology were counted in the intermediate zone (Figure 1E). Multipolar cells were defined as cells with more than three processes or polygonal morphology, and inverted bipolar as cells whose trailing process is thicker than leading process. Normal bipolar indicates locomoting neurons. Graph in Figure 1D shows the ratio of cells with branched leading process to locomoting neurons ± SEM. (n = 4 brains). Cells without leading process or inverted bipolar morphology were excluded in the analysis in Figure 1D. See also the Supplemental Experimental Procedures for details.

Quantitative Estimation of Perinuclear N-Cadherin Accumulation

Primary cortical neurons (2 DIV) were immunostained with anti-N-cadherin and anti-EGFP antibodies. The fluorescent signals of N-cadherin at perinuclear regions and other cytoplasmic regions (near the plasma membrane) were measured by the use of Leica SP5 software. To subtract the effects of cytoplasmic volume, EGFP fluorescent signals at the same regions were also measured and the ratio of N-cadherin to EGFP fluorescent signals was calculated to evaluate "corrected" N-cadherin signals. The ratio of the corrected N-cadherin signals in perinuclear regions to that of other cytoplasmic regions (near the plasma membrane) was evaluated (Figures 5C and 5F).

In addition, the ratio of cells with perinuclear N-cadherin accumulation was also evaluated (Figures 5G and S6D). The criterion for "perinuclear N-cadherin accumulation" is the high fluorescence intensity of N-cadherin at the perinuclear region, which was defined by Leica SP5 software (see Figures S6A and S6B). See the Supplemental Experimental Procedures for details.

Immunohistochemistry and Immunocytochemistry

Immunohistochemistry and immunocytochemistry were performed as described previously (Kawauchi et al., 2003, 2006). See the Supplemental Experimental Procedures for details.

Coculture of Primary Neurons and Nestin-Positive Cells

We modified a glial culture method and neuron-glial interaction assay developed by E.S. Anton and colleagues (Anton et al., 1999; Cameron et al., 1997; Gongidi et al., 2004). E15 mouse embryonic cerebral cortices were dissociated into single cells. Cells were suspended in 500 μl of minimum essential medium (MEM) containing 10% horse serum and plated on six-well dishes coated with 1 mg/ml poly-D-lysine (Sigma). After a 7 day culture with two passages, Tuj1-negative and Nestin-positive cells were concentrated. Subsequently, primary cortical neurons from E15 embryonic cerebral cortices were added to Nestin-positive cells and co-cultured in MEM containing 10% horse serum for 2 days. See also the Supplemental Experimental Procedures for details.

FACS Analysis

Primary cortical neurons transfected with Rab5-shRNA or control shRNA plus EGFP-expressing vectors were washed with ice-cold PBS, treated with anti-N-cadherin or β1-integrin antibody and incubated for 1 hr on ice. Cells were washed with PBS, treated with phycoerythrin-conjugated secondary antibody for 30 min on ice, and harvested with a cell scraper. After centrifugation at 2300 rpm (500G) for 5 min, cells were washed with PBS containing 0.1% bovine serum albumin and subjected to FACS analysis.

Rac1 Activation Assay (GST-PAK1 Pull-Down Assay)

GST-PAK1 pull-down assay was performed using Rac1 activation assay biochem kit (Cytoskeleton) according to the manufacturer's instructions. See the Supplemental Experimental Procedures for details.

Primary Culture of Embryonic Cortical Neurons and Immunoblotting

Primary culture experiments and immunoblotting were performed as described previously (Kawauchi et al., 2003). See the Supplemental Experimental Procedures for details.

SUPPLEMENTAL INFORMATION

Supplemental Information includes Experimental Procedures, references, and eight figures and can be found online at doi:10.1016/j.neuron.2010.07.007.

ACKNOWLEDGMENTS

We thank T. Baba, C. Bucci, S. Hirai, R. L. Huganir, S. Kanda, B. J. Knoll, D. Manor, M. McCaffrey, F. D. Miller, J. Miyazaki, M. Ozawa, R. E. Pagano, K. Takei, K. Tanabe, and D. L. Turner for providing plasmids, Kaori Kawauchi for a part of statistical analyses, and Ruth T. Yu and Akira Sakakibara for helpful comments. We also thank the Core Instrumentation Facility, Keio University School of Medicine for help with Leica SP5 confocal microscopy, LAS4000mini, FACS and ABI DNA sequencer. This work was supported by Grants-in-Aid from the Ministry of Education, Culture, Sports, and Science and Technology, Japan (#21113524 to T.K., #19670002 to M.H., and #22240041 to K.N.), and by grants from the JST PRESTO program, Takeda Science Foundation and GCOE. Author contributions; T.K. conceived the study and designed and performed experiments. K.S., M.S., and K.C. performed experiments. K.T. partly performed N-cadherin knockdown. K.K. constructed a part of N-cadherin vectors. Y.N., M.H., K.N., and T.K. administrated the experimental environments. T.K. jointly wrote the paper with M.H.

Accepted: June 23, 2010
Published: August 25, 2010

REFERENCES

Altschuler, Y., Barbas, S.M., Terlecky, L.J., Tang, K., Hardy, S., Mostov, K.E., and Schmid, S.L. (1998). Redundant and distinct functions for dynamin-1 and dynamin-2 isoforms. J. Cell Biol. *143*, 1871–1881.

Anton, E.S., Kreidberg, J.A., and Rakic, P. (1999). Distinct functions of alpha3 and alpha(v) integrin receptors in neuronal migration and laminar organization of the cerebral cortex. Neuron *22*, 277–289.

Ayala, R., Shu, T., and Tsai, L.H. (2007). Trekking across the brain: the journey of neuronal migration. Cell *128*, 29–43.

Cameron, R.S., Ruffin, J.W., Cho, N.K., Cameron, P.L., and Rakic, P. (1997). Developmental expression, pattern of distribution, and effect on cell

aggregation implicate a neuron-glial junctional domain protein in neuronal migration. J. Comp. Neurol. *387*, 467–488.

Damke, H., Baba, T., Warnock, D.E., and Schmid, S.L. (1994). Induction of mutant dynamin specifically blocks endocytic coated vesicle formation. J. Cell Biol. *127*, 915–934.

Ezratty, E.J., Partridge, M.A., and Gundersen, G.G. (2005). Microtubule-induced focal adhesion disassembly is mediated by dynamin and focal adhesion kinase. Nat. Cell Biol. *7*, 581–590.

Ezratty, E.J., Bertaux, C., Marcantonio, E.E., and Gundersen, G.G. (2009). Clathrin mediates integrin endocytosis for focal adhesion disassembly in migrating cells. J. Cell Biol. *187*, 733–747.

Ferguson, S.M., Raimondi, A., Paradise, S., Shen, H., Mesaki, K., Ferguson, A., Destaing, O., Ko, G., Takasaki, J., Cremona, O., et al. (2009). Coordinated actions of actin and BAR proteins upstream of dynamin at endocytic clathrin-coated pits. Dev. Cell *17*, 811–822.

Gleeson, J.G., and Walsh, C.A. (2000). Neuronal migration disorders: from genetic diseases to developmental mechanisms. Trends Neurosci. *23*, 352–359.

Gloster, A., Wu, W., Speelman, A., Weiss, S., Causing, C., Pozniak, C., Reynolds, B., Chang, E., Toma, J.G., and Miller, F.D. (1994). The T alpha 1 alpha-tubulin promoter specifies gene expression as a function of neuronal growth and regeneration in transgenic mice. J. Neurosci. *14*, 7319–7330.

Gongidi, V., Ring, C., Moody, M., Brekken, R., Sage, E.H., Rakic, P., and Anton, E.S. (2004). SPARC-like 1 regulates the terminal phase of radial glia-guided migration in the cerebral cortex. Neuron *41*, 57–69.

Guerrier, S., Coutinho-Budd, J., Sassa, T., Gresset, A., Jordan, N.V., Chen, K., Jin, W.L., Frost, A., and Polleux, F. (2009). The F-BAR domain of srGAP2 induces membrane protrusions required for neuronal migration and morphogenesis. Cell *138*, 990–1004.

Hatanaka, Y., and Murakami, F. (2002). In vitro analysis of the origin, migratory behavior, and maturation of cortical pyramidal cells. J. Comp. Neurol. *454*, 1–14.

Hirai, S., Kawaguchi, A., Hirasawa, R., Baba, M., Ohnishi, T., and Ohno, S. (2002). MAPK-upstream protein kinase (MUK) regulates the radial migration of immature neurons in telencephalon of mouse embryo. Development *129*, 4483–4495.

Huang, C., Jacobson, K., and Schaller, M.D. (2004). MAP kinases and cell migration. J. Cell Sci. *117*, 4619–4628.

Kadowaki, M., Nakamura, S., Machon, O., Krauss, S., Radice, G.L., and Takeichi, M. (2007). N-cadherin mediates cortical organization in the mouse brain. Dev. Biol. *304*, 22–33.

Kawauchi, T., and Hoshino, M. (2008). Molecular pathways regulating cytoskeletal organization and morphological changes in migrating neurons. Dev. Neurosci. *30*, 36–46.

Kawauchi, T., Chihama, K., Nabeshima, Y., and Hoshino, M. (2003). The in vivo roles of STEF/Tiam1, Rac1 and JNK in cortical neuronal migration. EMBO J. *22*, 4190–4201.

Kawauchi, T., Chihama, K., Nishimura, Y.V., Nabeshima, Y., and Hoshino, M. (2005). MAP1B phosphorylation is differentially regulated by Cdk5/p35, Cdk5/p25, and JNK. Biochem. Biophys. Res. Commun. *331*, 50–55.

Kawauchi, T., Chihama, K., Nabeshima, Y., and Hoshino, M. (2006). Cdk5 phosphorylates and stabilizes p27kip1 contributing to actin organization and cortical neuronal migration. Nat. Cell Biol. *8*, 17–26.

Lock, J.G., and Stow, J.L. (2005). Rab11 in recycling endosomes regulates the sorting and basolateral transport of E-cadherin. Mol. Biol. Cell *16*, 1744–1755.

LoTurco, J.J., and Bai, J. (2006). The multipolar stage and disruptions in neuronal migration. Trends Neurosci. *29*, 407–413.

Martinez-Cerdeno, V., Noctor, S.C., and Kriegstein, A.R. (2006). The role of intermediate progenitor cells in the evolutionary expansion of the cerebral cortex. Cereb. Cortex *16* (*Suppl 1*), i152–i161.

Nadarajah, B., Brunstrom, J.E., Grutzendler, J., Wong, R.O., and Pearlman, A.L. (2001). Two modes of radial migration in early development of the cerebral cortex. Nat. Neurosci. *4*, 143–150.

Nishimura, T., and Kaibuchi, K. (2007). Numb controls integrin endocytosis for directional cell migration with aPKC and PAR-3. Dev. Cell *13*, 15–28.

Nishimura, Y.V., Sekine, K., Chihama, K., Nakajima, K., Hoshino, M., Nabeshima, Y., and Kawauchi, T. (2010). Dissecting the factors involved in the locomotion mode of neuronal migration in the developing cerebral cortex. J. Biol. Chem. *285*, 5878–5887.

Okamoto, P.M., Herskovits, J.S., and Vallee, R.B. (1997). Role of the basic, proline-rich region of dynamin in Src homology 3 domain binding and endocytosis. J. Biol. Chem. *272*, 11629–11635.

Olson, E.C., Kim, S., and Walsh, C.A. (2006). Impaired neuronal positioning and dendritogenesis in the neocortex after cell-autonomous Dab1 suppression. J. Neurosci. *26*, 1767–1775.

Palamidessi, A., Frittoli, E., Garre, M., Faretta, M., Mione, M., Testa, I., Diaspro, A., Lanzetti, L., Scita, G., and Di Fiore, P.P. (2008). Endocytic trafficking of Rac is required for the spatial restriction of signaling in cell migration. Cell *134*, 135–147.

Pelkmans, L., Fava, E., Grabner, H., Hannus, M., Habermann, B., Krausz, E., and Zerial, M. (2005). Genome-wide analysis of human kinases in clathrin- and caveolae/raft-mediated endocytosis. Nature *436*, 78–86.

Pereira-Leal, J.B., and Seabra, M.C. (2001). Evolution of the Rab family of small GTP-binding proteins. J. Mol. Biol. *313*, 889–901.

Pfeffer, S.R. (2001). Rab GTPases: specifying and deciphering organelle identity and function. Trends Cell Biol. *11*, 487–491.

Praefcke, G.J., and McMahon, H.T. (2004). The dynamin superfamily: universal membrane tubulation and fission molecules? Nat. Rev. Mol. Cell Biol. *5*, 133–147.

Rakic, P. (1972). Mode of cell migration to the superficial layers of fetal monkey neocortex. J. Comp. Neurol. *145*, 61–83.

Rakic, P. (2009). Evolution of the neocortex: a perspective from developmental biology. Nat. Rev. Neurosci. *10*, 724–735.

Raman, M., Chen, W., and Cobb, M.H. (2007). Differential regulation and properties of MAPKs. Oncogene *26*, 3100–3112.

Romero Rosales, K., Peralta, E.R., Guenther, G.G., Wong, S.Y., and Edinger, A.L. (2009). Rab7 activation by growth factor withdrawal contributes to the induction of apoptosis. Mol. Biol. Cell *20*, 2831–2840.

Rosenfeld, J.L., Moore, R.H., Zimmer, K.P., Alpizar-Foster, E., Dai, W., Zarka, M.N., and Knoll, B.J. (2001). Lysosome proteins are redistributed during expression of a GTP-hydrolysis-defective rab5a. J. Cell Sci. *114*, 4499–4508.

Saito, T., and Nakatsuji, N. (2001). Efficient gene transfer into the embryonic mouse brain using in vivo electroporation. Dev. Biol. *240*, 237–246.

Schaar, B.T., and McConnell, S.K. (2005). Cytoskeletal coordination during neuronal migration. Proc. Natl. Acad. Sci. USA *102*, 13652–13657.

Sheen, V.L., Ganesh, V.S., Topcu, M., Sebire, G., Bodell, A., Hill, R.S., Grant, P.E., Shugart, Y.Y., Imitola, J., Khoury, S.J., et al. (2004). Mutations in ARFGEF2 implicate vesicle trafficking in neural progenitor proliferation and migration in the human cerebral cortex. Nat. Genet. *36*, 69–76.

Shin, H.W., Morinaga, N., Noda, M., and Nakayama, K. (2004). BIG2, a guanine nucleotide exchange factor for ADP-ribosylation factors: its localization to recycling endosomes and implication in the endosome integrity. Mol. Biol. Cell *15*, 5283–5294.

Shintani, Y., Fukumoto, Y., Chaika, N., Svoboda, R., Wheelock, M.J., and Johnson, K.R. (2008). Collagen I-mediated up-regulation of N-cadherin requires cooperative signals from integrins and discoidin domain receptor 1. J. Cell Biol. *180*, 1277–1289.

Stenmark, H., and Olkkonen, V.M. (2001). The Rab GTPase family. Genome Biol. *2*, reviews3007.1–reviews3007.7.

Tabata, H., and Nakajima, K. (2001). Efficient in utero gene transfer system to the developing mouse brain using electroporation: visualization of neuronal migration in the developing cortex. Neuroscience *103*, 865–872.

Tabata, H., and Nakajima, K. (2003). Multipolar migration: the third mode of radial neuronal migration in the developing cerebral cortex. J. Neurosci. *23*, 9996–10001.

Tabata, H., Kanatani, S., and Nakajima, K. (2009). Differences of migratory behavior between direct progeny of apical progenitors and basal progenitors in the developing cerebral cortex. Cereb. Cortex *19*, 2092–2105.

Takahashi, T., Goto, T., Miyama, S., Nowakowski, R.S., and Caviness, V.S., Jr. (1999). Sequence of neuron origin and neocortical laminar fate: relation to cell cycle of origin in the developing murine cerebral wall. J. Neurosci. *19*, 10357–10371.

Teckchandani, A., Toida, N., Goodchild, J., Henderson, C., Watts, J., Wollscheid, B., and Cooper, J.A. (2009). Quantitative proteomics identifies a Dab2/integrin module regulating cell migration. J. Cell Biol. *186*, 99–111.

Tissir, F., and Goffinet, A.M. (2003). Reelin and brain development. Nat. Rev. Neurosci. *4*, 496–505.

Tsai, L.H., and Gleeson, J.G. (2005). Nucleokinesis in neuronal migration. Neuron *46*, 383–388.

Xie, Z., Sanada, K., Samuels, B.A., Shih, H., and Tsai, L.H. (2003). Serine 732 phosphorylation of FAK by Cdk5 is important for microtubule organization, nuclear movement, and neuronal migration. Cell *114*, 469–482.

Yano, H., Mazaki, Y., Kurokawa, K., Hanks, S.K., Matsuda, M., and Sabe, H. (2004). Roles played by a subset of integrin signaling molecules in cadherin-based cell-cell adhesion. J. Cell Biol. *166*, 283–295.

Zerial, M., and McBride, H. (2001). Rab proteins as membrane organizers. Nat. Rev. Mol. Cell Biol. *2*, 107–117.

Zhang, J., Woodhead, G.J., Swaminathan, S.K., Noles, S.R., McQuinn, E.R., Pisarek, A.J., Stocker, A.M., Mutch, C.A., Funatsu, N., and Chenn, A. (2010). Cortical neural precursors inhibit their own differentiation via N-cadherin maintenance of beta-catenin signaling. Dev. Cell *18*, 472–479.